# Color Constancy For Improving Skin Detection

**A. Nadian-Ghomsheh** *a_nadian@sbu.ac.ir*
*Cyberspace research group,*
*Shahid Beheshti University, GC*
*Tehran, 1983963113, Iran*

**Abstract**

Skin detection is a preliminary step in many human related recognition systems. Most skin detection systems suffer from high false detection rate, resulting from low variance between the skin and non-skin color distributions. This paper proposes the use of simple color correction algorithms with low computation complexity to obtain a corrected version of the skin color distribution, which could lead to more accurate skin detection. White patch retinex, Grey world assumption and several improved versions of these two state of the art correction algorithms were chosen and applied to an image set of 4000. The results, compared with skin detection with no color correction revealed that color correction will improve the skin detection accuracy.

**Keywords:** Skin Detection, Color Constancy, Gaussian Distribution, White Patch Retinex, Grey World Assumption.

## 1. INTRODUCTION

Human skin is widely used in image processing research related to humans, with applications in areas such as face detection [1], person tracking [2], pornography filtering [3], and steganography [4]. Recent approaches for skin detection are focused on skin color information, since it is an invariant feature against rotation and scaling [5].

Visible spectrum imaging has been the focus for skin detection in most research. This is a challenging task due to various factors such as illumination, camera characteristics, ethnicity, and added facial components. Basically, skin detection can be considered as classification of skin pixels and non-skin pixels. Three steps have to be considered for skin detection: choice of a proper color space, modeling skin and non-skin pixels with a suitable model, and classification of the modeled distributions.

Many color spaces have been considered for skin detection. Basic color spaces such as the RGB and normalized RGB (nRGB) have shown to be very attractive for skin detection since RGB is the default color space for many available image formats [6-8]. Perceptual color spaces, such as HSV, HSI, HSL, and TSL are another group of color spaces that have been used for skin detection extensively [9-11]. Transforming for RGB to such color spaces is invariant to high intensity, surface orientation and ambient light which makes these color space attractive for skin detection. However, perceptual feature of these group of color spaces, such as hue and saturation cannot be directly converted from a RGB space, and many transformation that do so are based on non-linear equations which could increase the computation time for skin detection. Orthogonal color space, such as YCbCr, YIQ, YUV and YES on the other hand are transformed into RGB space using linear transformations [12-14]. Using this group of color spaces, it is possible to separate the luminance component of a color space from its chrominance component. This is a great advantage when considering a color space for skin detection, because omitting the luminance in an image will help to achieve a skin color distribution independent of scene illumination [15].

Detecting skin pixels can be viewed as a two class problem, where, skin pixels are grouped against the non-skin pixels. In general, two approached are considered for skin detection: pixel-based skin detection and regional-based skin detection. Pixel-based skin detection uses the pixel color information for detecting skin pixels, where as regional methods use the information of an ensemble of pixels to detect the skin region [16].

Pixel-based methods use the color information from a large number of training skin pixels to obtain the skin color distribution used to detect skin pixels [15, 17]. In some methods, explicit rules were used to detect the skin region for naked image detection [18, 19]. Although this approach executes very fast, it suffers from lack of accuracy [20]. Histogram-based Gaussian mixture model was used by [21]. In this method, the processing time increases dramatically as the number of Gaussians is increased. Lee [22] used a learning-based chromatic distribution-matching scheme to determine the image's skin chroma distribution online.

Regional-based methods use the relationship between pixels to detect the human skin. In the work of [18], after using explicit rules for skin detection, a region growing step was performed to refine the detected skin region. In the method of [23], skin pixels were detected by finding the skin color distribution from certain areas around the eyes. Adaptive methods have also been used for detecting skin pixels in arbitrary images [24-26]. These methods are dependent on the information within each image, rather than the initial skin color distribution. However, if the adaptation step requires an intense iterative process, computation time increases dramatically.

In general, pixel-based skin detection suffers from low accuracy [15, 27, 28]. On the other hand, regional methods have shown to be more accurate compared to pixel-based methods [26, 29]. However, simplicity of implementation and low computational cost, makes pixel-based skin detection more widely used in applications that require skin detection.

In this paper we try to improve the skin detection accuracy using color constancy. Color constancy is integrated with the Gaussian model for skin detection. The focus of this study is to investigate the effectiveness of simple to implement color constancy algorithms for improving the accuracy of skin detection. White Patch Retinex (WPR) algorithm, the Grey World (GA) assumption and some of their variations are considered as color correction algorithms. The skin image database used in this paper was a collection of 4000 images divided into two equal sets of skin and non-skin images. The images were randomly chosen from the QOMPAC database[30].

The rest of the paper is organized as follows: in section two, color correction algorithms used in this paper are briefly explained. Section three explains the training and test phases of the skin detection procedure used in this paper. Experimental results are shown in section four and the paper is concluded in section five.

## 2. COLOR CORRECTION FOR SKIN DETECTION

Color is an important biological signalling mechanism, and without it, objects could no longer be reliably identified by their color [31]. There are two approaches to follow in developing color constancy algorithms. The first method is to determine the reflectance of objects. The second approach is to perform a color correction that closely mimics the performance of the visual system.

In our work, we consider the fact that different lighting situations and the camera settings will produce a skin color distribution map that is different when compared to a color corrected version. By correcting the colors in images, it is possible to obtain a skin color distribution that is more similar to the true skin color distribution. Thus, the objective of this study is not focused on finding a color correction algorithm that is closer to what human visual system expects, but to find a correction algorithm that is more suited for distinguishing between skin pixels and pixels that show the same color properties as skin. This similarity could be the result of scene illumination or the camera calibration. Figure 1a shows a scene at sunset. It is clear that the colors in this image

are very close to the color of human skin, mostly due to the illumination of the scene. Figure1b shows the same image corrected with the Multi Scale Retinex with Color Restoration (MSRCR) [32] method. The output of the color correction algorithm might not be considered as a good picture, but the output image of this algorithm clearly changes the skin-like colors, so that most of the pixels in the output image do not have colors which are close to the color of the human skin. On the other hand, in Figures 1c and 1d, it's shown that the pixels that belong to the face region, still resemble the color of the skin after applying MSRCR. This examples shows how color constancy can be used in favour of improving the accuracy of skin detection.

There are many color constancy algorithms available ranging from very simple algorithms such as WP algorithm and some more complex and sophisticated algorithms that are capable of handling the correction of poorly colored images such as method presented in [33, 34]. In this study, the desired algorithm is the one that is executed fast and has the capability of correcting images with various lighting situations up to an expectable level. For this reason, we have chosen two main approaches: the WP algorithm and some improved versions of this method. The Gray World assumption (GW) algorithm has also been considered in this paper. These methods are briefly explained in this section.

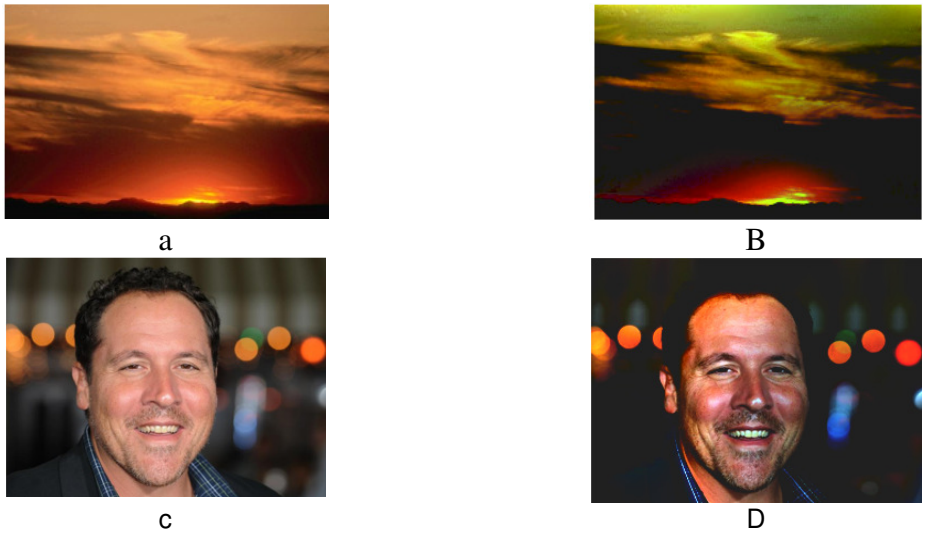


**FIGURE 1: a)** sun set scene and **b)** its corrected version. **c)** A skin image and its **d)** corrected version.

### 2.1 White Patch Retinex Method

The WP algorithm relies on having a bright patch somewhere in the image. The idea is that, if there is a white patch in the scene, then this patch reflects the maximum light possible for each band, which can be considered as the color of the illuminant.

In this model, the illuminant is considered to be uniform and the intensity at pixel position *(x,y)* for each color channel $i \in \{R,G,B\}$ representing the three color channels red, green and blue, is calculated by:

$$I_i(x, y) = G(x, y)R_i(x, y)L_i \quad (1)$$

where $G(x,y)$ is a factor that depends on the scene geometry at the corresponding object position, $R_i(x,y)$ is the reflectance for wavelength $\lambda_i$, and $L_i$ is the irradiance at wavelength $\lambda_i$. For WP it is assumed that $R_i(x,y)=1$ for all $i$, and $G(x,y)=1$. Since the maximum intensity values in each channel is considered, the color of illuminant is obtained by:

$$L_{i,\max} = \max_{x,y} \{c_i(x, y)\} \quad (2)$$

where $c$ is the color value of a pixel at position $(x,y)$ in the image. The color corrected image can obtained by normalizing the image by $L_{i,max}$:

$$O_i(x, y) = \frac{c_i(x, y)}{L_{i,\max}} \quad (3)$$

where $O$ is the output of the color correction algorithm for the $i^{th}$ channel. In the Modified White Patch Retinex (MWP) algorithm, the pixels that were used to find the maximum $L_{i,max}$ were chosen at a gray level less than the maximum saturated value [31]. Thus $L_{i,max}$ in (3) would be less than the actual maximum value in the image.

An improved version of WP was presented by [35], called the Single-Scale Retinex (SSR). In this algorithm, $L_i(x,y)$ is estimated by applying a Gaussian-form linear low pass filter to an input color image $c_i(x,y)$. $o_i(x,y)$, is then obtained by subtracting the log signal of the estimated illumination from the log signal of the input color image as follows:

$$o_i = \log c_i(x, y) - \log l_i(x, y) \quad (4)$$

This algorithm is shown to have trade-off between dynamic range compression and tonal rendition. Thus, improving each factor will cause a degradation on the other. Jobson, [36] further improved their work to overcome this problem be implementing the Multi-Scale Retinex (MSR). In this method the surround function is represented as:

$$o_i = \sum_{n=1}^{N} w_n O_{SSRni}(x, y) \quad (5)$$

where, $N$ represents the number of scales, $W_n$ represents the weight of each scale, and $O_{SSRni}$ are the outputs of the SSR algorithm. In the SSR and MSR algorithm, a color change in the output image may occur, because these algorithms are employed to color channels $i$ separately, and each channel is enhanced independently. In this algorithms, the number of bins that image should be quantized into, needs to be specified.

MSRCR was introduced by [32] to overcome these problems. In this method, the output image is calculated as:

$$o_i = WF_i O_{MSRi}(x, y) \quad (6)$$

where $O_{MSRi}$ is the output image from the MSR for channel $i$, and $WF_i$ is the weight function obtained via:

$$WF_i = b \log\left[ a \frac{O_{MSRi}(x, y)}{\sum_{j \in \{R,G,B\}} O_{MSRj}(x, y)} \right] \quad (7)$$

In the equation, $a$ and $b$ are the adjustment constants in this algorithm.

**2.2 Gray World Assumption**

The gray world color constancy algorithm assumes that the colors of the objects in view are

uniformly distributed over the entire color range and we have a sufficient number of objects with different colors in the scene, then the average color computed for each channel will be close to 0.5. The corrected image via the gray world assumption can be obtained by:

$$o_i(x,y) = \frac{c_i(x,y)}{fa_i} \tag{8}$$

where $f$ is a constant related to the expected value of the geometry factor $G$ and the and $a$ is the space color average of an image with size $n=nx\times ny$ obtained by:

$$a_i = \frac{1}{n} \sum_{x,y} c_i(x,y) \tag{9}$$

Using this notation, $a_i$ can be affected by the size of different objects in the scene. One way to overcome this problem is to calculate $a_i$ for a color segmented image [31]. Let $n_r$ be the number of different regions and let $a(R_j)=[a_R(R_j),a_G(R_j),a_B(R_j)]^T$ be the average color of region $J\epsilon\{1,\ldots,n_r\}$. Now, $a_i$ can be calculated by looping over the unique regions:

$$a_i = \frac{1}{n_r} \sum_{j=1}^{n_r} a_i(R_j) \tag{10}$$

This approach was further improved by using image histograms instead of using the segmented image. This was performed to avoid the redundant segments generated resulted from the position of objects in the scene. The resulting $a_i$ was calculated by:

$$a_i = \frac{1}{n_{nz}} \sum_{j=1}^{n_b} c_j(j) \tag{11}$$

were $n_b$ is the total of buckets used in the histogram, and $n_{nz}$ is the number of nonzero buckets.

## 3. SKIN DETECTION

To detect the skin pixels, it is required to choose a color space that skin pixels are well distributed within that space. Much research has been devoted to finding such a color space [5]. Although, no unique color space has been defined as the best choice for skin detection, two points can be noted: chrominance spaces provide sufficient information for skin detection, and YCbCr, normalized-RGB (nRGB), have been frequently reported as good choices for detecting skin pixels. Thus, these two spaces have been considered in this study. The block diagram of the skin detection process for the training and test phase implemented in this paper are shown in figure 2.

YCbCr color space is obtained from the RGB space by:

$$\begin{bmatrix} Y \\ Cb \\ Cr \end{bmatrix} = \begin{bmatrix} 16 \\ 128 \\ 128 \end{bmatrix} + \begin{bmatrix} 65.481 & 128.55 & 24.96 \\ -37.3 & -74.2 & 112 \\ 112 & -93.7 & -18.2 \end{bmatrix} \begin{bmatrix} R \\ G \\ B \end{bmatrix} \tag{12}$$

In this space, Cb and Cr color channels represent the chrominance information and are used for skin detection. nRGB space is obtained from RGB space via:

$$r = \frac{\mathrm{R}}{\mathrm{R}+\mathrm{G}+\mathrm{B}}, \quad g = \frac{G}{R+G+B}, \qquad b = \frac{B}{R+G+B} \tag{13}$$

Since r + g + b = 1 in (13), the information of one color channel will be redundant and can be ignored. In this paper, the color channels *r* and *g* channels have been considered for skin detection.

The Gaussian distribution was chosen for skin pixel classification. To implement the method, the skin color distribution obtained from the sample skin pixels were used to estimate the Gaussian distribution representing the skin class. In the test stage, the probability of each pixels was obtained via:

$$P_{Gaussian}(X \mid \mu, \Lambda) = \frac{1}{2\pi|\Lambda|^{0.5}} \exp^{-0.5(X-\mu)^T|\Lambda|^{-1}(x-\mu)} \tag{14}$$

were X is the input pixel, μ and Λ are the mean vector and covariance matrix of the skin distribution in the respective color space. Each pixel with $P_{Gaussian} > T$ is classified as skin.

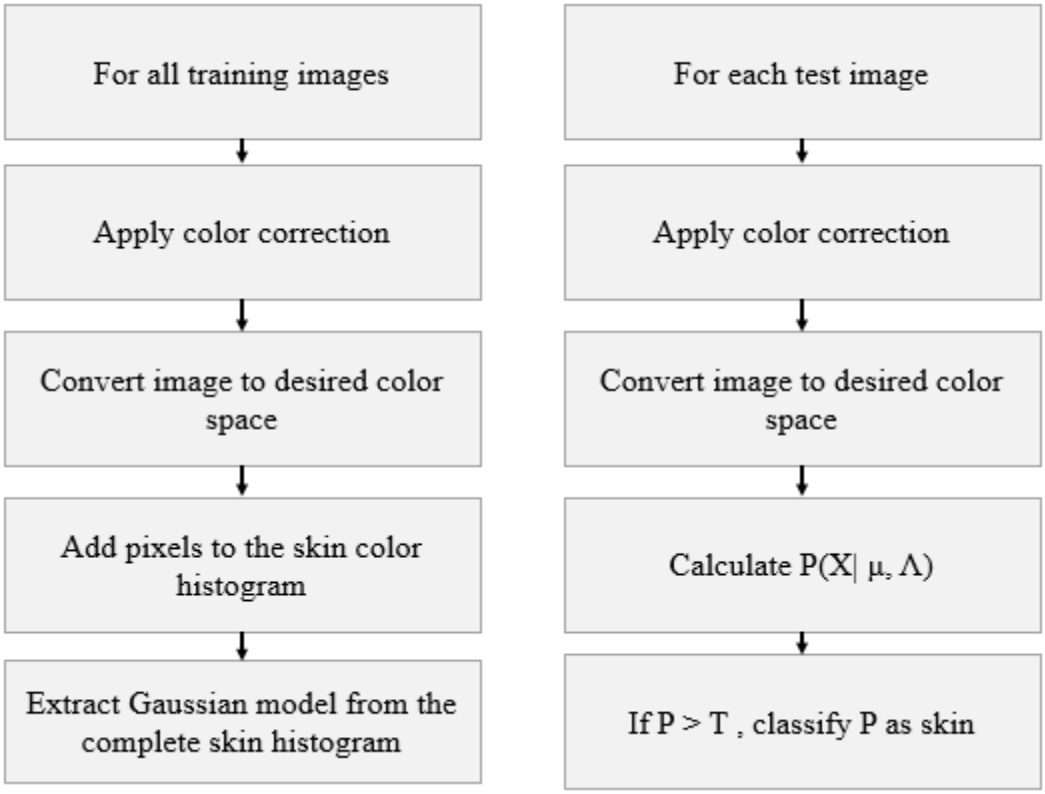


**FIGURE 2: Left.** Training process of skin detection. **Right.** Steps for skin detection.

## 4. EXPERIMENTAL RESULTS

This section reports the result of skin detection on color corrected images. The test data set used in this study was a collection of 2000 skin image and 2000 non-skin images, randomly chosen from the COMPAQ data base. In addition, 1000 test images were used to obtained skin color distribution in the training phase. Choosing two color spaces and several color constancy algorithms provide a large set of experimental scenarios. Some of the color constancy algorithm used in this paper require parameter settings which further increased the number of cases that

require to be experimented with.
For WP and the GW, no specific setting was required. Testing these algorithms on the YCbCr and nRGB spaces made four test cases. For the SSR and MSR algorithms, the number of bins that was used to build the image histogram needed to be considered. In this study histograms were build using {16, 32, 64, 128, 256} bins. Further, SSR and MSR were applied to the R channel, RGB channels, Y channel, and YCbCr channels from the RGB and YCbCr space separately, providing 40 test cases. The MWP algorithm was tested for 4 cases by choosing input entries {50, 100, 150, 200} as the threshold for finding the white patch in the image. For this algorithm, skin detection was applied using the YCbCr space. The MSRCR algorithm required three tuning parameters. By choosing three values for each entry as {a ϵ [2 5 7], b ϵ [2 5 7], scales ϵ [10 15 20]}, a total of 27 scenarios were required to be tested for this algorithm.

Figure 3 shows the result of color correction on two sample images. As this figure shows, applying color constancy algorithms influences both the skin color and the color of non-skin pixels. Although these changes might not favour the better appearance of an image, however, such changes might lead to a better skin detection result. For example, in the case of image correction with WP algorithm, the skin image has preserved its skin color, while the color of the non-skin image has totally changed. As another example, when MWP is applied to the sample images of figure 3, the colors in the non-skin image does not resemble the skin color after color correction, while, the skin image shows a color skin that looks more relevant with the human visual system after color correction. The result of skin detection for each case is shown in the following paragraphs of this section.


**FIGURE 3:** Applying color correction algorithms to two sample skin (left) and non-skin (right) images.

Figure 4 shows the skin color distribution of skin pixels in Cb-Cr space. As the figure indicates the skin color distribution is much different for each correction algorithm. Skin color distribution obtained from the WP, GW and MSR algorithms represent skin color distribution in a small region of the space when compared with the other three method.

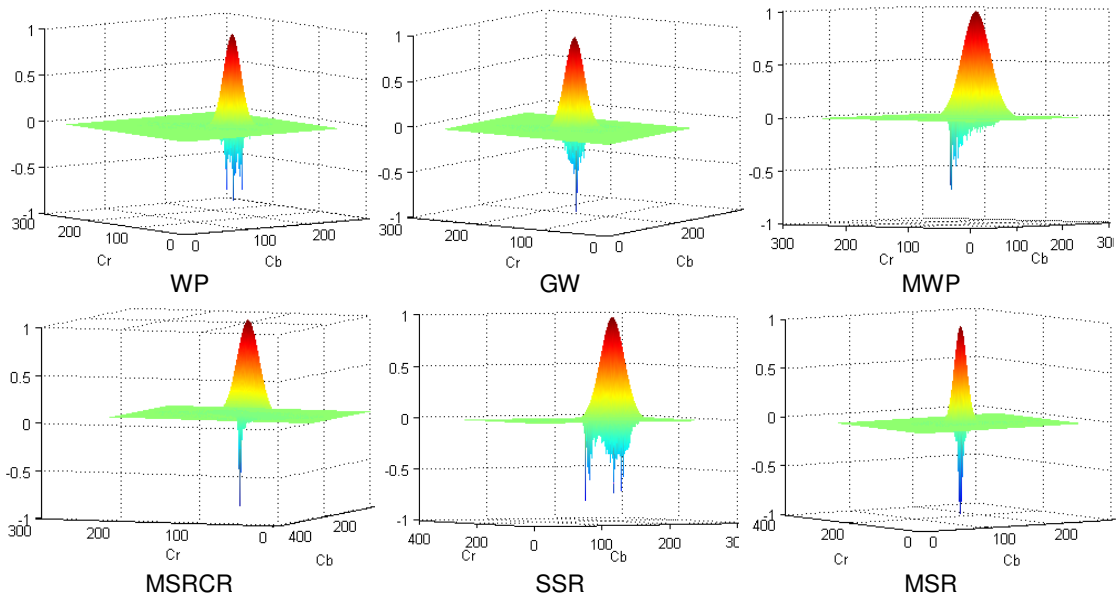


**FIGURE 4:** Skin color distribution after color correction in Cb-Cr chrominance space.

Although it might seem that MSR, WP, and GW algorithm should be better correction methods, but, their effect on non-skin images is unknown. To numerically evaluate the effectiveness of the color correction algorithm for improving skin detection accuracy, Recursive Operation Characteristic (ROC) curves were used based on the values of True Positive Rate (TPR) and

False Positive Rate (FPR) [30]. The accuracy of skin detection was obtained via:

$$Acc = \frac{TPR}{TPR + FPR} \tag{15}$$

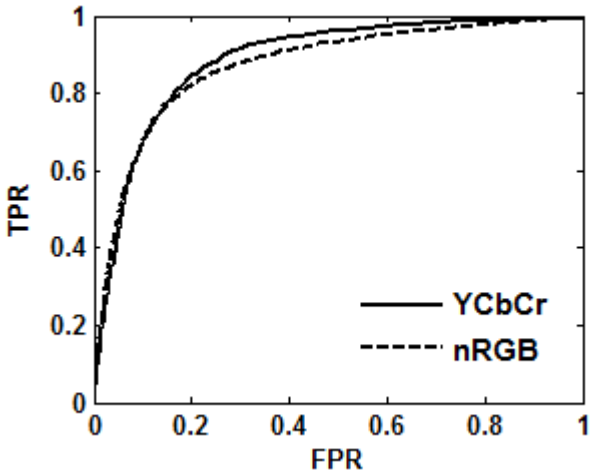


**FIGURE 5:** Result of skin detection before applying color constancy.

Figure 5 shows the result of skin detection before applying any color correction to the image data set. As this figure shows, the YCbCr color space yield better results when compared to that of the nRGB color space. Table 1 summarizes the FPR rates for TPR = 90% and 95%. As the table indicates, the YCbCr outperforms the nRGB space by 4.5% for TPR of 90%.

| | TPR(%) | FPR(%) | Accuracy(%) |
|---|---|---|---|
| YCbCr | 85 | 19 | 83 |
| nRGB | | 24 | 80 |
| YCbCr | 90 | 28 | 81 |
| nRGB | | 37 | 76.5 |

**TABLE 1:** Skin detection results without color correction.

Figure 6 shows the result of skin detection after applying the WP and GW color correction algorithms. As the results indicate, after applying color correction algorithms, the YCbCr algorithm outperforms the result of skin detection when using nRGB color space. Comparision between the two correction algorirhms reveal that the WP had better skin detection result. Table 2 shows the numerical results obtained from figure 6. An accuracy of 84.25% was obtained when skin detection was performed using Cb-Cr chrominance space and WP algorithm was used for color correction. The best result for skin detection in nRGB color space was 81.75%, which was obtained when WP algorithm was used for color correction.

| | | TPR(%) | FPR(%) | Accuracy(%) |
|---|---|---|---|---|
| WP | YCbCr | 85 | 17 | 84 |
| | nRGB | | 21.5 | 81.75 |
| | YCbCr | 90 | 21.5 | 84.25 |
| | nRGB | | 34.5 | 77.75 |
| GW | YCbCr | 85 | 19 | 83.75 |
| | nRGB | | 22 | 81.5 |
| | YCbCr | 90 | 26.5 | 81.75 |
| | nRGB | | 35 | 77.5 |

**TABLE 2:** Skin detection results for applying WP and GW algorithms.

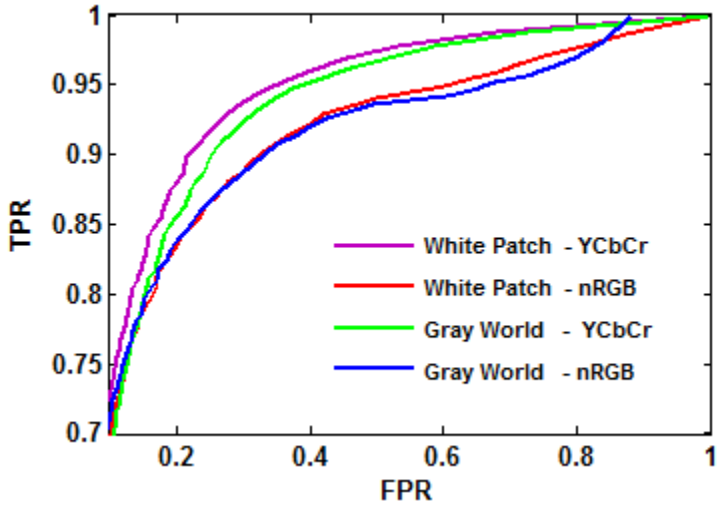


**FIGURE 6:** Result of skin detection after applying WP and the GW.

The skin detection ROC curves obtained after applying the SSR algorithm are shown in figure 7. Each figure is captioned as $X_c$-$Y_s$, where $X_c$ shows which color channels were corrected and $Y_s$ show which color space was used for skin detection. X ϵ {R, RGB, Y, YCbCr} and Y ϵ {nRGB, YCbCr}. For figure 7a through 7d, the color correction was applied to the color channels of the RGB space, where, the best ROC curves for applying SSR algorithm was obtained. The figure also indicates that correction of color in the YCbCr space has a negative effect on the skin detection accuracy. For the case where SSR was applied to all color channels of the YCbCr space, the skin detection accuracies were dramatically decreased to unacceptable levels.

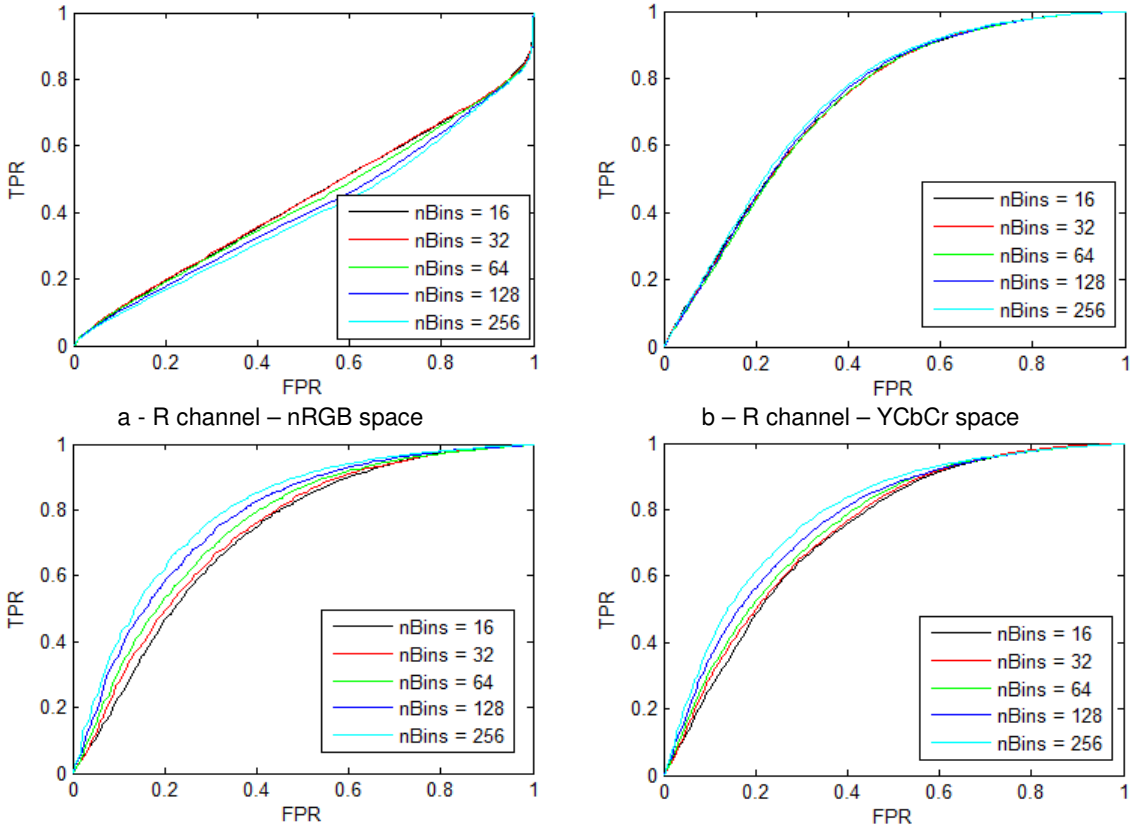


a - R channel – nRGB space

b – R channel – YCbCr space

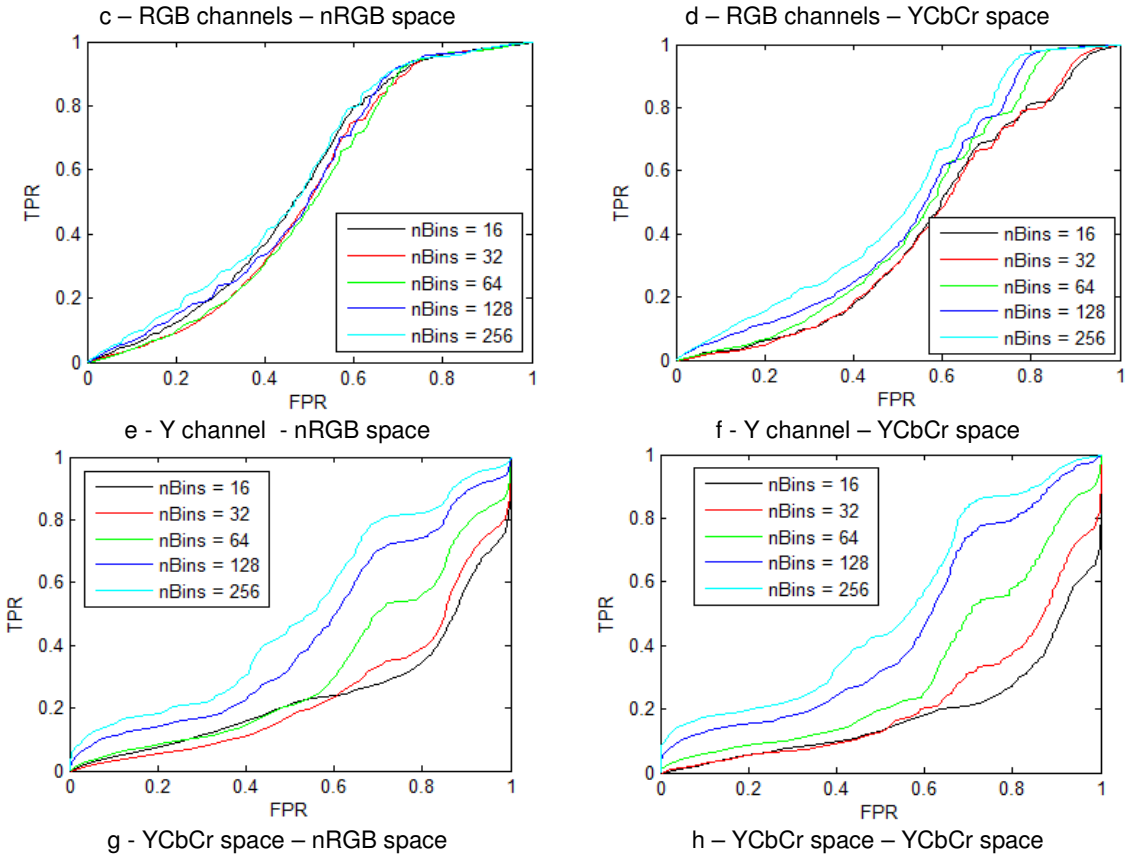


**FIGURE 7:** The ROC curves obtained from different scenarios when SSR algorithm was used for color correction.

Table 3 shows the results of skin detection obtained from the ROC curves of figure 7. As the results in this table indicate, none of the scenarios have improved the skin detection accuracy. However, among the tested scenarios, when color constancy was applied to all channels of the RGB color space, an accuracy of 73.5% was obtained. In this case, nRGB color space was used for skin detection.

| | Color space | Number of bins | Corrected channel | TPR(%) | FPR(%) | Accuracy(%) |
|---|---|---|---|---|---|---|
| Single – Scale Retinex | nRGB | 128 | R | 85 | 85 | 50 |
| | | | RGB | 85 | 38 | 73.5 |
| | | 64 | R | 85 | 80 | 52.5 |
| | | | RGB | 85 | 42 | 71.5 |
| | YCbCr | 128 | R | 85 | 47 | 69 |
| | | | RGB | 85 | 41 | 72 |
| | | 64 | R | 85 | 46.5 | 69.25 |
| | | | RGB | 85 | 44 | 70.5 |

**TABLE 3:** Skin detection accuracy using SSR for color correction.

Figure 8 shows the result of skin detection when MSR algorithm was used for color correction. The figures are labelled in the same manner as the result of skin detection with SSR algorithm. As the figure indicates, for correcting YCbCr color channels unacceptable results was obtained, as it was the case with the SSR algorithm. Table 4 shows some of the results obtained when MSR algorithm was applied for color correction. As the table indicates, the best result was

obtained when color constancy algorithm was applied to all the channels of the RGB color space, where an accuracy of 73.5% was obtained,

| | Color space | Number of bins | Corrected channel | TPR(%) | FPR(%) | Accuracy (%) |
|---|---|---|---|---|---|---|
| Multi – Scale Retinex | nRGB | 64 | R | 85 | 43 | 71 |
| | | 64 | RGB | 85 | 41 | 72 |
| | | 128 | R | 85 | 43 | 71 |
| | | 128 | RGB | 85 | 38 | 73.5 |
| | YCbCr | 64 | R | 85 | 45 | 70 |
| | | 64 | RGB | 85 | 44 | 70.5 |
| | | 128 | R | 85 | 44 | 70.5 |
| | | 128 | RGB | 85 | 42 | 71.5 |

**TABLE 4:** Skin detection accuracy using MSR for color correction.

When MWP algorithm was used for color correction, the ROC curves shown in figure 9 where obtained. As this figure indicates, for threshold 150 and 200, acceptable ROC curves were obtained. Table 3 summarizes the result of skin detection after applying the MWP for color correction. As shown in the table, choosing a threshold of 200 resulted in skin detection with accuracy of 86.25% for TPR = 85%. In the case for TPR = 90%, an accuracy of 86% percent was obtained. This result indicates that MWP had better performance compared with the WP algorithm, because for the WP, the saturated value is used for luminance estimation and in most cases a single fully saturated point might decrease the performance of the algorithm.

| | Threshold | TPR(%) | FPR(%) | Accuracy(%) |
|---|---|---|---|---|
| MWP | 200 | 85 | 12.5 | 86.25 |
| | | 90 | 18 | 86 |
| | | 95 | 27 | 84 |
| | 150 | 85 | 23.5 | 80.75 |
| | | 90 | 31 | 79.5 |
| | | 95 | 45 | 75 |

**TABLE 5:** Skin detection accuracy results after applying the MWP.

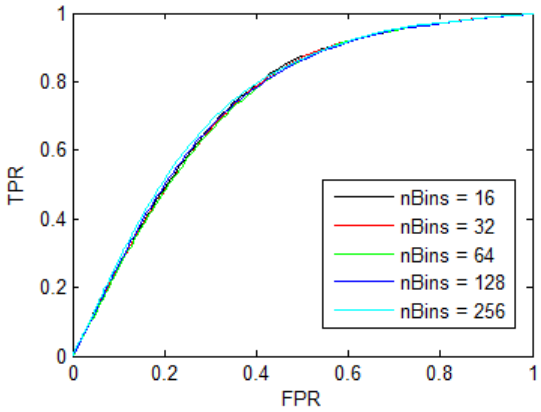


a – R channel - nRGB space

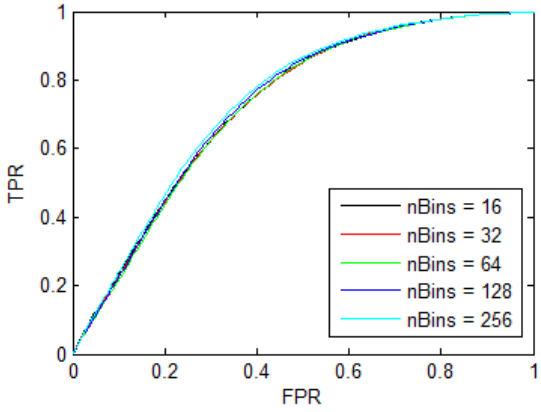


b – R channel - YCbCr space

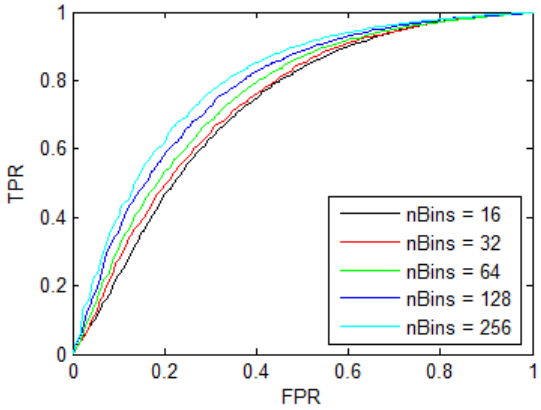


c – RGB channels - nRGB space

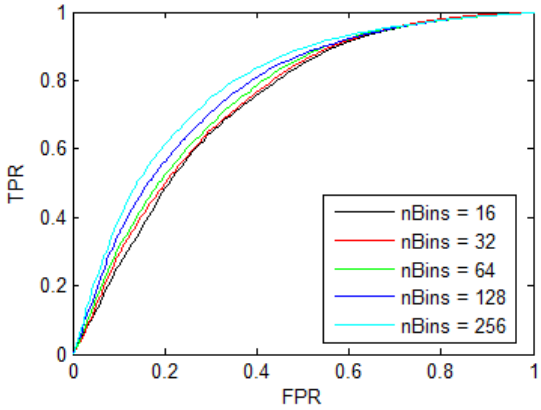


d – RGB channels - YCbCr space

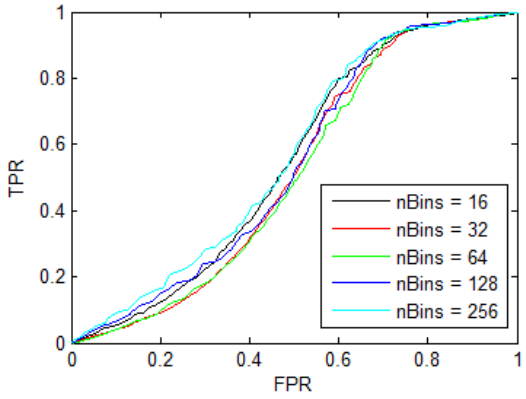


e – Y channel - nRGB space

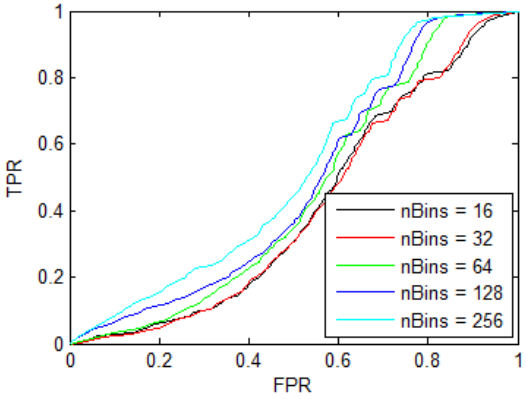


f – Y channel - YCbCr space

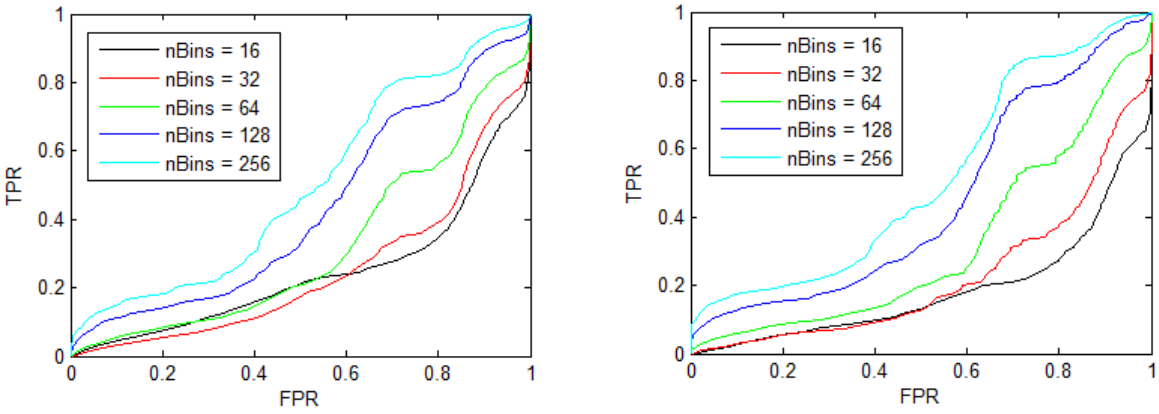


g – YCbCr Channels - nRGB space

h – YCbCr channels - YCbCr space

**FIGURE 8:** The skin detection ROC curves obtained from different settings of MSR.

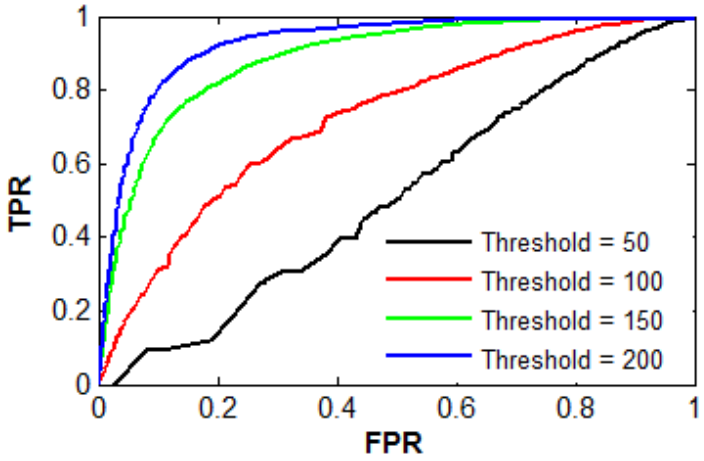


**FIGURE 9:** The result of skin detection after applying the MWP algorithm.

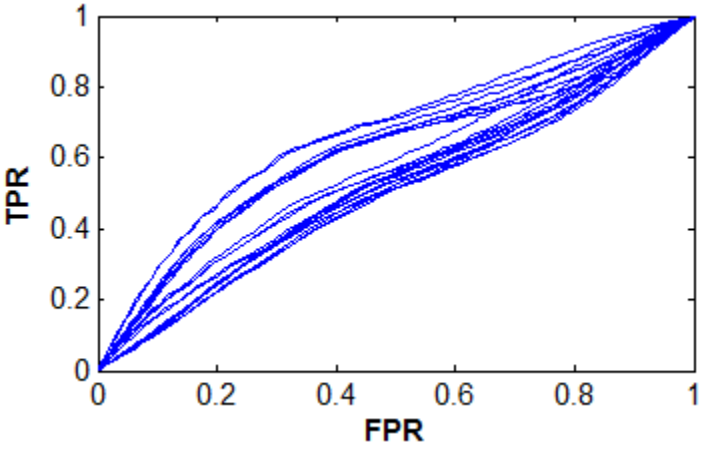


**FIGURE 10:** Skin detection ROC curves after applying the MSRCR color correction algorithm.

For the case of image correction using the MSRCR algorithm, unacceptable results were obtained. In the best case the accuracy did not exceed 70%. Figure 10 shows the skin detection ROC curves obtained for different test scenarios.

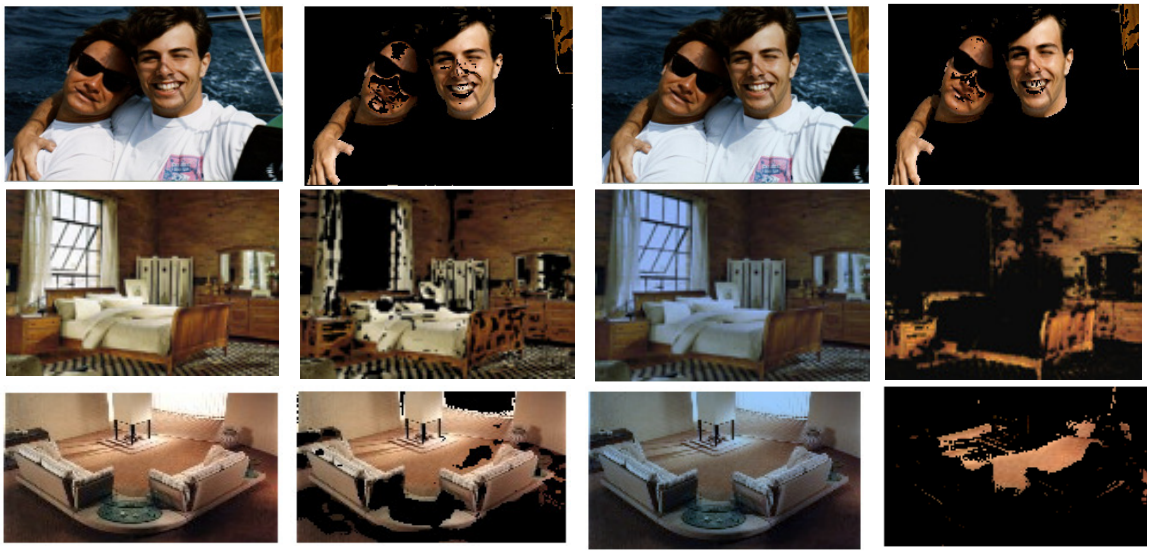

a b c d

**FIGURE 11:** Examples of detected skin region after applying MWP color correction algorithm. a) Original image, b) skin region detected without color correction, c) color correction image, and d) detected skin region after color correction.

Figure 11 shows the result of skin detection for three samples images. The detected skin region before color correction, the color corrected image and the detected skin region after color correction are shown for each image. The images were color corrected using the MWP algorithm. For the skin image, the detected skin region is slightly improved. For the non-skin images, the number of pixels that have been incorrectly classified as skin are significantly reduced. This results confirms with the main idea of this paper, where, it was suggested that correcting the color of images will produce a more reliable skin color distribution map, and many non-skin images after color correction will produce colors that are different with the human skin color.

Figure 12 compares the result of skin detection without color correction against scenarios were color correction was applied to images prior to skin detection. Only, the result of cases with accuracy greater than that obtained from the skin detection with no color correction are reported in this figure. Overall, WP, GW, and the MWP algorithms showed to be effective for improving skin detection, and color correction using MWP improved the skin detection accuracy by more than 3%.

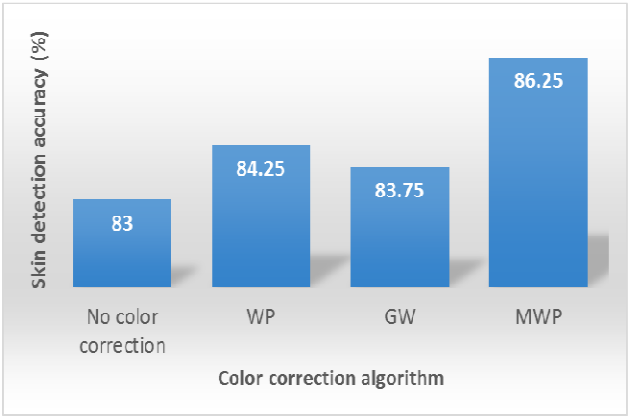


**FIGURE 12:** Comparison between different skin detection accuracies.

## 5. CONCLUSION

In this paper, we proposed the use of simple color correction algorithms for improving skin detection accuracy. Several versions of the WP and the GW algorithms were used for color correction and their results were tested against skin detection with no color correction. The results showed that applying the WP and GW prior the skin detection will improved the result of skin detection. Further, the MWP algorithm was the most efficient method for improving skin detection accuracy among the color correction algorithms tested in this paper. Using MWP, a skin detection accuracy of 86.25% was obtained which was an improvement to skin detection without color correction by 3.25%. The various results reported in this paper confirmed that applying simple color correction algorithms prior to skin detection can improve the skin detection accuracy. Future research on color constancy for improving skin detection can be focused on finding color correction algorithms that are especially tailored for the application of skin detection. Overall, MWP was simple to implement and did not require complex computation for obtaining color correction, this algorithm is suitable for improving skin detection accuracy.

## 6. REFERENCES

[1] OJO, J.A. and S.A. Adeniran, Colour face image database for skin segmentation, face detection, recognition and tracking of Black faces under real-life situations. International Journal of Image Processing (IJIP), 2011. 4(6): p. 600.

[2] Choi, W., C. Pantofaru, and S. Savarese, A general framework for tracking multiple people from a moving camera. Pattern Analysis and Machine Intelligence, IEEE Transactions on, 2013. 35(7): p. 1577-1591.

[3] Nadian, A. and A. Talebpour, A New Skin Detection Approach for Adult Image Identification. Research Journal of Applied Sciences, Engineering and Technology, 2012. 4(21): p. 4535-4545.

[4] Shejul, A.A. and U.L. Kulkarni, A secure skin tone based steganography using wavelet transform. International Journal of computer theory and Engineering, 2011. 3(1): p. 16-22.

[5] Kakumanu, P., S. Makrogiannis, and N. Bourbakis, A survey of skin-color modeling and detection methods. Pattern recognition, 2007. 40(3): p. 1106-1122.

[6] Yang, M.-H. and N. Ahuja. Gaussian mixture model for human skin color and its application in image and video databases. in Proc. SPIE: Storage and Retrieval for Image and Video Databases VII. 1999.

[7] Bergasa, L.M., et al., Unsupervised and adaptive Gaussian skin-color model. Image and Vision Computing, 2000. 18(12): p. 987-1003.

[8] Soriano, M., et al., Adaptive skin color modeling using the skin locus for selecting training pixels. Pattern Recognition, 2003. 36(3): p. 681-690.

[9] Wang, Y. and B. Yuan, A novel approach for human face detection from color images under complex background. Pattern Recognition, 2001. 34(10): p. 1983-1992.

[10] Mohammed, K., B.C. Ennehar, and T. Yamina, Skin detection using gaussian mixture models in YCbCr and HSV color space. Global Journal on Technology, 2012. 1.

[11] Berbar, M.A., Skin colour correction and faces detection techniques based on HSL and R colour components. International Journal of Signal and Imaging Systems Engineering, 2014. 7(2): p. 104-115.

[12] Cao, X.Y. and H.F. Liu, A skin detection algorithm based on Bayes decision in the YCbCr color space. Applied Mechanics and Materials, 2012. 121: p. 672-676.

[13] Tao, L., et al. A circuit of configurable skin tone adjusting method base on exact skin color region detection. in Electron Devices and Solid-State Circuits (EDSSC), 2011 International Conference of. 2011. IEEE.

[14] Al Tairi, Z.H. and M.I. Saripan, Skin segmentation using YUV and RGB color spaces. Journal of information processing systems, 2014. 10(2): p. 283-299.

[15] Nadian, A. and A. Talebpour. Pixel-based skin detection using sinc function. in Computers & Informatics (ISCI), 2011 IEEE Symposium on. 2011. IEEE.

[16] Nadian, A., A. Talebpour, and M. Basseri. Regional skin detection based on eliminating skin-like lambertian surfaces. in Computers & Informatics (ISCI), 2011 IEEE Symposium on. 2011. IEEE.

[17] Jedynak, B., H. Zheng, and M. Daoudi. Statistical models for skin detection. in Computer Vision and Pattern Recognition Workshop, 2003. CVPRW'03. Conference on. 2003. IEEE.

[18] Hammami, M., Y. Chahir, and L. Chen, Webguard: A web filtering engine combining textual, structural, and visual content-based analysis. Knowledge and Data Engineering, IEEE Transactions on, 2006. 18(2): p. 272-284.

[19] Shih, J.-L., C.-H. Lee, and C.-S. Yang, An adult image identification system employing image retrieval technique. Pattern Recognition Letters, 2007. 28(16): p. 2367-2374.

[20] Vezhnevets, V., V. Sazonov, and A. Andreeva. A survey on pixel-based skin color detection techniques. in Proc. Graphicon. 2003. Moscow, Russia.

[21] Hu, W., et al., Recognition of pornographic web pages by classifying texts and images. Pattern Analysis and Machine Intelligence, IEEE Transactions on, 2007. 29(6): p. 1019-1034.

[22] Lee, J.-S., et al., Naked image detection based on adaptive and extensible skin color model. Pattern recognition, 2007. 40(8): p. 2261-2270.

[23] Jang, S.-W., et al., An adult image identification system based on robust skin segmentation. Journal of Imaging Science and Technology, 2011. 55(2): p. 20508-1.

[24] Cho, K.-M., J.-H. Jang, and K.-S. Hong, Adaptive skin-color filter. Pattern Recognition, 2001. 34(5): p. 1067-1073.

[25] Kawulok, M., J. Kawulok, and J. Nalepa, Spatial-based skin detection using discriminative skin-presence features. Pattern Recognition Letters, 2014. 41: p. 3-13.

[26] Sun, H.-M., Skin detection for single images using dynamic skin color modeling. Pattern recognition, 2010. 43(4): p. 1413-1420.

[27] Do, H.-C., J.-Y. You, and S.-I. Chien, Skin color detection through estimation and conversion of illuminant color under various illuminations. Consumer Electronics, IEEE Transactions on, 2007. 53(3): p. 1103-1108.

[28] Shoyaib, M., et al., Skin detection using statistics of small amount of training data. Electronics letters, 2012. 48(2): p. 87-88.

[29] Cheddad, A., et al., A skin tone detection algorithm for an adaptive approach to steganography. Signal Processing, 2009. 89(12): p. 2465-2478.

[30] Jones, M.J. and J.M. Rehg, Statistical color models with application to skin detection. International Journal of Computer Vision, 2002. 46(1): p. 81-96.

[31] Ebner, M., Color constancy. Vol. 6. 2007: John Wiley & Sons.

[32] Rahman, Z.-u., D.J. Jobson, and G.A. Woodell. Resiliency of the multiscale retinex image enhancement algorithm. in Color and Imaging Conference. 1998. Society for Imaging Science and Technology.

[33] Ebner, M. and J. Hansen, Depth map color constancy. Bio-Algorithms and Med-Systems, 2013. 9(4): p. 167-177.

[34] Gijsenij, A., T. Gevers, and J. Van De Weijer, Generalized gamut mapping using image derivative structures for color constancy. International Journal of Computer Vision, 2010. 86(2-3): p. 127-139.

[35] Jobson, D.J., Z.-U. Rahman, and G.A. Woodell, Properties and performance of a center/surround retinex. Image Processing, IEEE Transactions on, 1997. 6(3): p. 451-462.

[36] Jobson, D.J., Z.-U. Rahman, and G.A. Woodell, A multiscale retinex for bridging the gap between color images and the human observation of scenes. Image Processing, IEEE Transactions on, 1997. 6(7): p. 965-976.